MODELING AND EXPLOITING CHANNEL VARIABILITY OF WIRELESS NETWORKS

A Dissertation Outline Presented

by

ANAND SEETHARAM

Submitted to the Graduate School of the
University of Massachusetts Amherst in partial fulfillment
of the requirements for the degree of

DOCTOR OF PHILOSOPHY

August 2012

Computer Science

MODELING AND EXPLOITING CHANNEL VARIABILITY OF WIRELESS NETWORKS

A Dissertation Outline Presented

by

ANAND SEETHARAM

Approved as to style and content by:

Jim Kurose, Chair

Don Towsley, Member

Arun Venkataramani, Member

Dennis Goeckel, Member

Lori Clarke, Department Chair
Computer Science

To amma, appa, akka and Arti

ACKNOWLEDGMENTS

ABSTRACT

MODELING AND EXPLOITING CHANNEL VARIABILITY OF WIRELESS NETWORKS

AUGUST 2012

ANAND SEETHARAM

B.E., JADAVPUR UNIVERSITY

M.Sc., UNIVERSITY OF MASSACHUSETTS AMHERST

Ph.D., UNIVERSITY OF MASSACHUSETTS AMHERST

Directed by: Professor Jim Kurose

The temporal and spatial variation in wireless channel conditions makes it challenging to design protocols for wireless networks. In this thesis, this variability is explicitly modeled at the coarse timescale, and variations at multiple timescales are taken into account in the design of efficient protocols for both end-to-end data forwarding in general, and for video distribution in particular. In the first part of the thesis, we model and analyze two classes of routing protocols - opportunism and cooperation, under varying channel conditions and in the presence of interfering transmitters.

In the second part of the thesis we investigate mobile scenarios and study the impact of both mobility and changing link quality on the performance of these networks. We first consider the problem of modeling coarse timescale channel variation in wireless networks and develop a shadowing-based Markov chain model to this end. We next present the design and analysis of a base-station scheduling algorithm that takes

both channel variability and varying bit rate of videos to into account, delivering streaming videos to users with the aim of minimizing the number of application-playout stalls. Last, we present an analysis of the tradeoff between the amount of signaling overhead incurred in path selection in a MANET with time-varying wireless channels and the application-level throughput and end-to-end power expended on the selected path.

TABLE OF CONTENTS

LIST OF TABLES

Table **Page**

LIST OF FIGURES

Figure **Page**

INTRODUCTION

0.1 Variability in Wireless Networks

The temporal and spatial variation in wireless channel conditions makes it challenging to design protocols for wireless networks. In order to architect efficient and robust protocols, it is essential to understand the inherent characteristics of wireless networks such as connectivity, channel variability, interference and coverage. Factors such as multipath fading, path loss and shadowing cause wireless channel variability at different timescales. Node mobility also plays an important role in determining wireless channel variability. In this thesis, our goal is to model the variability and to then exploit this variability and the broadcast nature of the wireless channel to improve user-level performance. We explore a wide range of wireless networks, both static and mobile, in this context.

The last decade has witnessed the growth and deployment of diverse networks such as mesh, ad-hoc, 4G, WiFi and WiMAX for various commercial and military purposes. One major question still remains unanswered: *How can one leverage the variability of the wireless channel to improve the application-level performance of clients using these networks?* We seek to answer this question by developing models for coarse timescale wireless channel variation and then designing and studying protocols that take advantage of wireless channel properties (such as multipath fading, shadowing and path loss) to make important decisions related to resource scheduling and network state information collection. In the following chapters we discuss our research results to date, as well as future work to be done as part of this dissertation.

0.2 Thesis Overview

To answer the question posed in the previous section we begin by providing a brief overview of the factors causing channel variability - multipath fading, path loss and shadowing and the different timescales at which they act. Multipath fading is caused by the destructive and constructive interference of the multipath waves and occurs in the milliseconds timescale. Path loss is the deterministic distance dependent component of the received power. Hence path loss fluctuations occur only in mobile scenarios and their variations occur mainly in the seconds to tens of seconds timescale, depending on client mobility. Shadowing is the variation in signal strength at the seconds timescale caused by large objects (e.g. buildings, trees) between the transmitter and receiver and is typically modeled as being independent of the distance between the transmitter and receiver.

The first part of the thesis analyzes the performance impact of multipath fading on link quality in static networks. We model and analyze two classes of routing protocols - opportunism and cooperation, under varying channel conditions and in the presence of interfering transmitters. In the second part of the thesis we investigate the impact of both mobility and changing link quality on the performance of wireless networks. To improve application-level performance over mobile wireless networks it is of prime importance to model coarse timescale channel variation. To achieve this, we first develop a Markov chain model for shadowing to capture its effect on received power. We then explore a video streaming setting where coarse timescale channel modeling and prediction is required and develop a scheduling algorithm to enhance the users' viewing experience. We are currently analyzing the tradeoff between the amount of signaling overhead incurred in path selection in a MANET with time-varying wireless channels and the application-level throughput and end-to-end power expended on the selected path.

The broadcast nature of wireless communication allows a much richer set of approaches to be taken when forwarding packets between source and destination than traditional hop-by-hop forwarding along pre-specified paths. These strategies fall

into two broad categories - opportunistic forwarding, which exploits relay diversity by opportunistically selecting an overhearing relay as a forwarder, and cooperative forwarding, which relies on the synchronized transmissions of relays to reinforce received signal strengths. In Chapter 1, our objective is to understand which among these two approaches provides higher performance (throughput) in presence of multiple competing and interfering network flows. We observe that opportunism outperforms cooperation and identify interference resulting from the larger number of transmissions under cooperative forwarding as a cause for mitigating the potential gains achievable with cooperative forwarding.

In the second part of the thesis, we focus primarily on mobile scenarios and concentrate on modeling and predicting power changes in wireless networks, and then using these predictions in resource allocation protocols. In Chapter 2 we develop a Markov chain model based on shadowing to model coarse time scale (seconds) on the received power and propose analytical and empirical techniques to determine the transition matrix of the Markov chain. We then conduct experiments over a WiMAX network and validate the abstract model by comparing its steady state and transient performance predictions with those computed using the empirically-derived transition matrix and those observed in the actual traces themselves.

A video streaming application is considered in Chapter 3 where we investigate multiplexing schemes to transmit multiple video streams from a base station to mobile clients with the objective of minimizing the number of playout stalls. We present an epoch-by-epoch framework to fairly allocate wireless transmission slots to streaming videos. First, we show that the problem of allocating slots fairly is NP-complete, even for a constant number of videos and then present a fast lead-aware greedy algorithm for the problem. Our trace-based evaluation shows that the greedy algorithm outperforms other algorithms both in terms of fairness and in terms of average number of stalls.

In dynamic network scenarios, it is advantageous to collect state information, provided that this information leads to better decisions that more than compensate for the additional overhead incurred. For example, the decrease in available path bandwidth as a result of state gathering overhead may be more than compensated for by the choice of better paths for routing data packets. Hence, in the last chapter of this dissertation we examine the tradeoff between amount of state information collected (at what precision, how often?) and overhead incurred, and the resulting performance (end-to-end power consumption for data and control traffic) in wireless networks while providing goodput guarantees. Understanding the tradeoff between the cost incurred in state information collection in a network and the resulting performance is a fundamental, yet largely unexplored problem. To date we have formulated a power optimization problem with goodput constraints and are currently investigating the number of bits per sample and state update frequency tradeoff numerically and via simulation.

0.3 Thesis Contributions

Having provided an overview of the thesis work in the previous section, we enumerate the main contributions of our research:

1. We show that opportunism outperforms cooperative forwarding and identify interference as the main cause for mitigating the potential gains achievable with cooperative forwarding.

2. We design a Markov chain model to capture the effect of shadowing on the received power. We develop analytical and empirical approaches to compute its transition matrix and show via experiments over a WiMAX network that the steady state and transient state performance of the Markov chain is close to that observed from real traces. We are currently designing a Kalman filter to predict received power variations at coarse timescales, with the expectation

that it will effectively capture the effect of both shadowing and path loss on the received power.

3. We design a greedy algorithm for scheduling multiple video streams from a base-station to mobile clients and show that our approach is fair and is successful in minimizing the number of application-playout stalls.

4. We use an information-theoretic bounding approach to quantitatively analyze the tradeoff between state information collection (sampling frequency and number of bits per sample) and power consumption. We intend to demonstrate that small number of bits per sample will carry very little information about the network while large number of bits per sample will carry marginal additional information. We believe that a similar tradeoff will exist for the sampling frequency as well.

The rest of the thesis proposal is structured as follows. We compare opportunistic and cooperative forwarding using generic assumptions in Chapter 1. In Chapter 2 we present a Markov chain model to model power variations in wireless networks. The problem of scheduling multiple videos (simultaneously being streamed from a base station to different mobile clients) so as to minimize the total number of playout stalls is studied in Chapter 3 and we propose a greedy algorithm to address this issue. We investigate the tradeoff between network state information collection and power consumption in wireless networks in Chapter 4. Chapter 5 concludes this proposal, summarizes planned future work, and sketches a completion time-line.

CHAPTER 1

OPPORTUNISM VS COOPERATION

1.1 Introduction

A wide range of forwarding strategies have been developed for multi-hop wireless networks, considering the broadcast nature of the wireless medium and the presence of random fading that results in time-varying and unreliable transmission quality. Two recently proposed strategies are opportunistic forwarding, which exploits relay diversity by opportunistically selecting an overhearing relay as a forwarder, and cooperative forwarding, which relies on the synchronized transmissions of relays to reinforce received signal strengths.

Although these strategies are well-known in the literature, there lacks a comparative analysis of their network-level performance in a realistic SINR (signal-to-interference-and-noise ratio) setting. Most extant work either focuses on link-level analysis in one-hop networks using a complicated channel fading model (e.g., [22,38]), or multi-hop network-level analysis using a very simple channel fading model (e.g., [4,6]). In the absence of a realistic model of random fading, the performance results obtained by the modeling and analysis of opportunistic and cooperative forwarding will not reflect the real-world performance.

In this chapter, we compare the performance of idealized and representative opportunistic and cooperative forwarding strategies under common (and realistic) assumptions. We stress that our goal here is *not* to propose new protocols or investigate a specific opportunistic or cooperative transmission protocol in detail. Instead, our more fundamental goal is to characterize and understand the differences between these two approaches to forwarding in various multi-hop wireless scenarios in presence of multiple competing flows.

In this chapter, we develop Markov chain models for these protocols, considering multiple competing flows in a general network setting. We first evaluate these models in simple small-scale networks, finding that opportunism often outperforms cooperation - a result corroborated by simulations in more general network settings. We also propose an approximate fixed-point model to efficiently compute the throughput of the Markov chain performance models in large networks. We identify interference resulting from the larger number of transmissions under cooperative forwarding as a cause for mitigating the potential gains achievable with cooperative forwarding.

The rest of the chapter is organized as follows. We briefly describe the forwarding strategies in Sec. 1.3. The wireless communication model is presented in Sec. 1.4. We present a Markov chain model in Sec. 1.5 and then study general topologies via simulation. In Sec 1.6, we provide the approximate fixed-point iteration for solving the Markov chain model.

1.2 Related Work

One of the earliest studies describing opportunistic forwarding appeared in [4]. Since then, a number of papers improved the practical benefits of opportunism [7, 29, 35, 59]. Research efforts have also theoretically analyzed the benefits of opportunism, including [28], where the authors performed a Markov chain analysis to determine the expected number of network-wide link-layer transmissions (ETX) needed to transfer a packet from source to destination in a wireless mesh network. Their work mostly assumes that link success probabilities are provided *a priori* and does not consider random fading in a SINR model, which is an important component of our models. Also, [6] provides a recursive relation for estimating the minimum number of required opportunistic transmissions. Similarly, [5] proposes an analytical model to study the performance (ETX) of opportunistic routing protocols. However, we remark that none of these papers consider a realistic SINR model with random fading.

There is also a considerable amount of research that considers cooperation in wireless networks. [38] and [22] summarize much of this prior work in cooperative diversity and demonstrate how cooperation improves network performance. However, most past research on cooperation has been in the context of the physical layer, with only a few efforts exploring how cooperation interacts with higher network layers [38]. In [11] the authors discuss how to effectively schedule cooperative transmissions for multiple access scenarios by helping sources with poor channels to the destination use relays that have better channel quality. We note that our work differs from prior work in that we address primarily the network-layer concern (with multihop forwarding), with the goal of comparing opportunistic forwarding and cooperative forwarding – using a simple model of SINR with random fading, and in a multihop setting.

1.3 Forwarding Strategies

This section describes the two forwarding strategies compared in this work - opportunistic forwarding and cooperative forwarding. We focus on generic and representative approaches, rather than the details, implementation and optimizations possible in any one specific approach.

Opportunistic Forwarding: If a packet cannot reach the destination in one hop, it is relayed by the overhearing node closest to the destination [4]. This process proceeds in multiple steps, until the packet reaches the destination. In the literature, there are proposals [4, 25] to address implementation issues, such as the selection of the appropriate relay when multiple nodes overhear the transmission. We abstract away implementation detail, and focus on the performance analysis of an ideal implementation in order to shed insights.

Cooperative Forwarding: To exploit the additive property of wireless signals, multiple overhearing relays can simultaneously transmit a packet towards the destination, when proper synchronization (e.g., by GPS) among multiple transmitters is feasible. We suppose that a flow maintains a list of relays. When a node belonging to a list of

relays of a particular flow overhears the transmission from the flow, it will be assigned as a relay. In the case of multiple network flows, we do not assume that nodes are allowed to coordinate their transmissions with other nodes that receive packets from other flows, as this would involve prohibitively high overhead. In this case, competing flows are essentially treated as interference.

1.4 Wireless Communication Model

In order to compare the performance of different forwarding strategies, we describe a model that accounts for SINR and random fading. Consider the general case with a set of cooperative transmitters T and a set of simultaneously competing transmitters I. Let the signal-to-interference-and-noise ratio be $\mathsf{S}^I_{T,j}$ which is defined as:

$$\mathsf{S}^I_{T,j} \triangleq \frac{\sum_{r\in T} |x_{r,j}|^2 \mathsf{P} d_{r,j}^{-\alpha}}{\mathsf{N_0} + \sum_{k\in I} |x_{k,j}|^2 \mathsf{P} d_{k,j}^{-\alpha}} \tag{1.1}$$

where $\mathsf{N_0}$ is a constant background noise, $|x_{i,j}|^2$ is the Rayleigh fading coefficient, $d_{i,j}$ is the distance between i and j, α is the path loss exponent, and P is the transmission power at i. Note that $d_{i,j} \geq 1$ and $\alpha \geq 2$. We assume that $|x_{i,j}|^2$ is an exponentially distributed i.i.d. random variable with normalized mean 1. We assume that a packet transmission is successful only if the SINR is above a threshold β. The probability that j can successfully receive the packet from a set of cooperative transmitters T in spite of interfering transmitters I is given by $P^I_{T,j} \triangleq \mathbb{P}\{\mathsf{S}^I_{T,j} \geq \beta\}$ and can be obtained from equation (1.2).

$$P^I_{T,j} = \sum_{r\in T}\sum_{k\in I} \frac{\exp\left(\frac{-\beta \mathsf{N_0}}{\mathsf{P} d_{r,j}^{-\alpha}}\right)}{\left(1+\beta(\frac{d_{r,j}}{d_{k,j}})^\alpha\right) \prod\limits_{r'\in T\setminus\{r\}} \left(1\text{-}(\frac{d_{r,j}}{d_{r',j}})^\alpha\right) \prod\limits_{k'\in I\setminus\{k\}} \left(1\text{-}(\frac{d_{k,j}}{d_{k',j}})^\alpha\right)} \tag{1.2}$$

1.5 Networks with Multiple Flows

In [40] we provide a detailed analysis of linear and diamond network topologies, considering a single flow, where we observe that the high-overhead cooperative for-

warding tends to perform marginally better that the lower-overhead opportunistic forwarding. However, when there are multiple competing flows in the network, the comparison becomes more subtle due to presence of interference, which mitigates the advantages of cooperative forwarding.

In this section we formulate Markov chain models to study a general setting with an arbitrary network topology and multiple flows. Using these Markov chain models, we first study a simple, small-scale grid topology analytically [8], and then use simulations for more general networks. We find that opportunistic forwarding can significantly outperform cooperative forwarding when inter-flow cooperation is not feasible. In the following, we consider the single packet case in which no new packet is transmitted by the source until the previous packet reaches the destination.

1.5.1 Opportunistic Forwarding

First, we present the Markov chain model for opportunistic forwarding in a general network topology and multiple flows. We denote a set of flows $\mathscr{F}$. Each flow $f \in \mathscr{F}$ has a priority list of participating nodes denoted by $\mathcal{P}_f = (v_{\mathrm{s}(f)}, v_1, ..., v_{\mathrm{d}(f)})$, where $v_{\mathrm{d}(f)}$ is the destination and $v_{\mathrm{s}(f)}$ is the source. Each succeeding node in $\mathcal{P}_f$ (e.g., v_i) has a higher priority than its preceding nodes (i.e., v_j for all $j < i$) for forwarding the packet, until the packet reaches $v_{\mathrm{d}(f)}$. Formally, we denote "$v_i \succ_f v_j$" to represent that v_i has a higher priority than v_j in $\mathcal{P}_f$ (e.g, it is 'closer' to the destination as in [4]). By a slight abuse of notation, we also denote $\mathcal{P}_f$ as a set of its listed members $\{v_{\mathrm{s}(f)}, v_1, ..., v_{\mathrm{d}(f)}\}$.

We denote the state of the network as $\vec{r} \triangleq (\vec{r}_f \in \mathcal{P}_f : f \in \mathscr{F})$, where $\vec{r}_f$ is the active relay for flow f for the next forwarding operation. We denote $\mathbf{P}_{\vec{r},\vec{r}'}$ the state transition probability from state $\vec{r}$ to state $\vec{r}'$, where ($\vec{r}'_f \succ_f \vec{r}_f$ or $\vec{r}'_f = \vec{r}_f$) and $\vec{r}'_f \neq v_{\mathrm{d}(f)}$, for at least one flow $f \in \mathscr{F}$. Let $\vec{r}_{\neg f} \triangleq \{\vec{r}_{f'} : f' \in \mathscr{F} \backslash \{f\}\}$. We obtain:

$$\mathbf{P}_{\vec{r},\vec{r}'} \triangleq \prod_{f \in \mathscr{F}} P^{\vec{r}_{\neg f}}_{\vec{r}_f,\vec{r}'_f} \cdot \prod_{v \in \mathcal{P}_f : v \succ_f \vec{r}'_f} (1 - P^{\vec{r}_{\neg f}}_{\vec{r}_f,v}) \tag{1.3}$$

where $P^{\vec{r}_{\neg f}}_{\vec{r}_f,\vec{r}'_f}$ can be obtained from (1.2) and $\mathbf{P}_{\vec{r},\vec{r}'}$ is the probability that every flow f receives a packet from active relay $\vec{r}_f$ to $\vec{r}'_f$, subject to the condition that the set of succeeding nodes $\{v \in \mathcal{P}_f : v \succ_f \vec{r}'_f\}$ that cannot receive the packet.

Recall that we assume an immediate transmission of a new packet after a successful delivery of a packet. Therefore when a flow reaches state $\vec{r}_f = v_{\mathrm{d}(f)}$ (i.e, the packet reaches the destination), the state transition in the next time step will correspond to the states reachable from the source with their respective probabilities. We can now evaluate the stationary distribution $\pi(\vec{r})$ for each state of the network $\vec{r}$ using (1.3). The throughput of each flow f, $\mathrm{T}_{\mathrm{gre}}(f)$, is given by:

$$\mathrm{T}_{\mathrm{opp}}(f) = \sum_{\vec{r}:\vec{r}_f = v_{\mathrm{d}(f)}} \pi(\vec{r}) \tag{1.4}$$

1.5.2 Cooperative Forwarding

For basic cooperative forwarding, we denote the state of the network as $\vec{R}$, where $\vec{R}_f \subseteq \mathcal{P}_f$ is a set of cooperative transmitters of flow f. Let $\vec{R}_{\neg f} \triangleq \bigcup_{f' \in \mathscr{F}\setminus\{f\}} \vec{R}_{f'}$. The state transition probability $\mathbf{P}_{\vec{R},\vec{R}'}$, where $\vec{R}_f \subseteq \vec{R}'_f$ and $v_{\mathrm{d}(f)} \notin \vec{R}_f$, is given by:

$$\mathbf{P}_{\vec{R},\vec{R}'} \triangleq \prod_{f \in \mathscr{F}} \prod_{v \in \vec{R}'_f \setminus \vec{R}_f} P^{\vec{R}_{\neg f}}_{\vec{R}_f,v} \cdot \prod_{v' \in \mathcal{P}_f \setminus \vec{R}'_f} \left(1 - P^{\vec{R}_{\neg f}}_{\vec{R}_f,v'}\right) \tag{1.5}$$

$P^{\vec{R}_{\neg f}}_{\vec{R}_f,v}$ can be obtained from (1.2). If the stationary distribution is denoted by $\pi(\vec{R})$, and the throughput of flow f, $\mathrm{T}_{\mathrm{co}}(f)$, is given by:

$$\mathrm{T}_{\mathrm{co}}(f) = \sum_{\vec{R},\vec{R}':v_{\mathrm{d}(f)} \in \vec{R}'_f} \pi(\vec{R}) \cdot \mathbf{P}_{\vec{R},\vec{R}'} \tag{1.6}$$

We studied a small scale grid topology and find that opportunistic forwarding can achieve higher throughput than cooperative forwarding [8]. We omit the analysis here, but the reader can consult [8].

1.5.3 Simulations for Random Networks

In this subsection we use simulation to study performance in larger network settings. As we will see, the insights gained in the small scale setting [8] generally apply in this more general setting as well. We consider 50 nodes uniformly distributed in a 100×100 area. For each simulation run, 4 distinct source-destination pairs are selected at random. We simulate the link quality between different pairs of nodes using the Rayleigh fading channel model. The simulation begins by all 4 sources transmitting packets. A node is able to receive a packet if the SINR between the transmitter and itself is above a threshold. The opportunistic and cooperative routing protocols determine the nodes that transmit packets in the next time slot. When a packet reaches the corresponding destination, the source starts transmitting a new packet. We keep track of the number of packets received at the destination. Each simulation run is performed for 2000 time units. We then determine the throughput for both opportunistic and cooperative forwarding strategies. Each point in Figure 1.1(a) is the value obtained for a particular run of the simulation.

For throughput comparisons, it is necessary to quantify the interference among packets flowing from source to destination along "paths" between given sets of source-destination pairs. Note, however, that there is no well-defined notion of a deterministic "path" along which packets flow for either opportunistic of cooperative forwarding. Further, as the position of the transmitters is unknown, we adopt an abstract approach to obtain a coarse measure of the interference. To characterize the interference among flows we take 10 points equidistantly-spaced between source and destination for each flow f; the i^{th} point is denoted by l_i^f. The interference between any two points is approximately modeled by the inverse of the distance raised to the path loss. For flow f, we consider the interference between each point l_i^f and all points $l_j^{f'}$ for every other flow f'. We repeat this process for each flow f and then add all of them together in the following manner:

$$\textsf{Intf-Metric} \triangleq \sum_{f\in\mathcal{F}} \sum_{f'\in\mathcal{F}\setminus\{f\}} \sum_{l_i^f} \sum_{l_j^{f'}} d_{l_j^{f'},l_i^f}^{-\alpha} \tag{1.7}$$

Intf-Metric therefore provides a coarse measure of the interference present in the network.

In Figure 1.1(a) we plot the difference in throughput between the opportunistic and cooperative strategies versus the Intf-Metric for an SINR threshold (β) of 3. Points above the line drawn at Throughput Difference=0 indicate the cases where opportunism performs better than cooperation while the nodes below the line depict the opposite. The figure shows that on average the performance of opportunism is better than that of cooperation for a wide range of Intf-Metric.

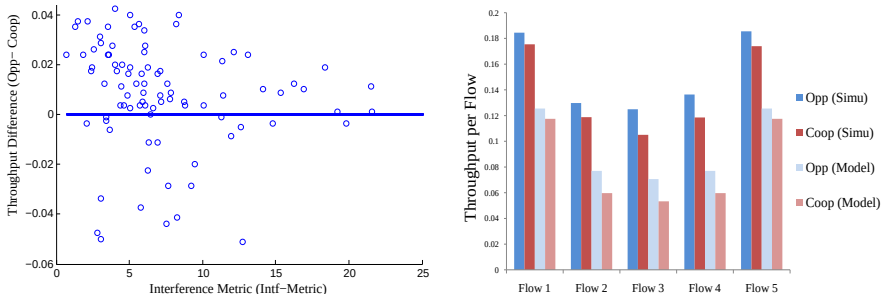

(a) Simulation of Random Network (b) Approximation vs. Simulation

Figure 1.1. Simulation and Fixed Point Approximation Results

1.6 Approximate Fixed-point Model

Sec. 1.5 provides an analysis of multiple flows in a general network setting. However, the number of states of the Markov chain increases exponentially with the number of flows. Hence, evaluating the stationary distributions of the Markov chain models quickly becomes intractable. Thus, in this section we introduce an approximate fixed-point model to simplify the evaluation, under the assumption of stationarity. We show that the throughput obtained from the approximate fixed-point model is generally lower them to the actual throughput of the Markov chain model. In the

approximate fixed-point model, we assume that the sets of participating nodes among distinct flows are disjoint (i.e., $\mathcal{P}_f \cap \mathcal{P}_{f'} = \varnothing$).

We approximate the stationary distributions by the Markov chains of individual flows separately, taking the expected interference from the other flows according to their stationary distributions. This gives rise to a set of fixed-point equations (one set for opportunistic forwarding and one set for cooperative forwarding) for the stationary distributions, which can be obtained via efficient iterative methods.

1.6.1 Opportunistic Forwarding

The state of a flow $f \in \mathscr{F}$ is specified by the active relay $r \in \mathcal{P}_f$ that overhears the transmission and has the highest priority among the overhearing participating nodes. We next describe a set of fixed-point equations considering individual flows. First, suppose that the stationary distribution of a node $j \in \mathcal{P}_f$ to be an active transmitting relay is given by $\hat{\pi}_f(j)$. Then, the expected interference to j from all other flows w.r.t. stationary distributions $\hat{\pi}_{\neg f} \triangleq \{\hat{\pi}_{f'} : f' \in \mathscr{F}\backslash\{f\}\}$ becomes (using the same notation as in (1.1):

$$\begin{aligned} \hat{I}_j^f(\hat{\pi}_{\neg f}) &= \sum_{f' \in \mathscr{F}\backslash\{f\}} \sum_{i \in \mathcal{P}_{f'}} \hat{\pi}_{f'}(j) \cdot \mathbb{E}[|x_{i,j}|^2] \cdot \mathsf{P} d_{i,j}^{-\alpha} \\ &= \sum_{f' \in \mathscr{F}\backslash\{f\}} \sum_{i \in \mathcal{P}_{f'}} \hat{\pi}_{f'}(j) \cdot \mathsf{P} d_{i,j}^{-\alpha} \end{aligned} \tag{1.8}$$

Note that $\hat{I}_j^f(\hat{\pi})$ does not depend on $\hat{\pi}_f$ itself, but only on $\{\hat{\pi}_{f'} : f' \in \mathscr{F}\backslash\{f\}\}$. Suppose that the interference from other flows remains stationary and has distribution $\hat{\pi}_{\neg f}$. Then the packet reception probability that j can successfully receive the packet from i in flow f w.r.t. $\hat{\pi}_{\neg f}$ is given by:

$$\hat{P}_{i,j}^f(\hat{\pi}_{\neg f}) \triangleq \mathbb{P}\Big\{ \frac{|x_{i,j}|^2 \mathsf{P} d_{i,j}^{-\alpha}}{\mathsf{N}_0 + \hat{I}_j^f(\hat{\pi}_{\neg f})} \geq \beta \Big\} = \exp\Big(\frac{-\beta\big(\mathsf{N}_0 + \hat{I}_j^f(\hat{\pi}_{\neg f})\big)}{\mathsf{P} d_{i,j}^{-\alpha}} \Big) \tag{1.9}$$

Next, we focus on the Markov chain of an individual flow. In such a Markov chain, we denote by $\hat{\mathbf{P}}_{r,r'}^f(\hat{\pi}_{\neg f})$ the state transition probability from an active relay $r \in \mathcal{P}_f$ to another active relay $r' \in \mathcal{P}_f$ such that ($r' \succ_f r$ or $r' = r$) and $r \neq v_{\mathrm{d}(f)}$, w.r.t. $\hat{\pi}_{\neg f}$:

$$\hat{\mathbf{P}}^{f}_{r,r'}(\hat{\pi}_{\neg f}) \triangleq \hat{P}^{f}_{r,r'}(\hat{\pi}_{\neg f}) \cdot \prod_{v \in \mathcal{P}_f : v \succ_f r'} \left(1 - \hat{P}^{f}_{r,v}(\hat{\pi}_{\neg f})\right) \tag{1.10}$$

The stationary distribution of such a Markov chain is $\hat{\pi}_f$, satisfying the following balance equations of for all $r \in \mathcal{P}_f$:

$$\sum_{r'' \in \mathcal{P}_f} \hat{\pi}_f(r) \cdot \hat{\mathbf{P}}^{f}_{r'',r}(\hat{\pi}_{\neg f}) = \sum_{r' \in \mathcal{P}_f} \hat{\pi}_f(r') \cdot \hat{\mathbf{P}}^{f}_{r,r'}(\hat{\pi}_{\neg f}) \tag{1.11}$$

subject to $\sum_{v \in \mathcal{P}_f} \hat{\pi}_f(v) = 1$. Equations (1.8)-(1.11) form a set of fixed-point equations for $(\hat{\pi}_f : f \in \mathscr{F})$. The fixed-point $(\hat{\pi}_f : f \in \mathscr{F})$ can be computed by an iterative method. We first assume a certain distribution $(\hat{\pi}^0_f : f \in \mathscr{F})$. Then we obtain $\hat{\pi}^1_f$ from Eqns. (1.8)-(1.11) w.r.t. $\hat{\pi}^0_{\neg f}$, for all $f \in \mathscr{F}$. We repeat the process for t steps, until $\hat{\pi}^t_f$ has a small deviation from $\hat{\pi}^{t-1}_f$. The throughput of the approximate fixed-point model is given by:

$$\hat{\mathrm{T}}_{\mathrm{opp}}(f) = \hat{\pi}_f(v_{\mathrm{d}(f)}) \tag{1.12}$$

1.6.2 Cooperative Forwarding

The approximate fixed-point model for basic cooperative forwarding is similar to that of opportunistic forwarding. In this case, however, the state of a flow is specified by the set of cooperative transmitters $R \subseteq \mathcal{P}_f$. From (1.2), the packet reception probability that j can successfully receive the packet from the set of cooperative transmitters R in a flow f is given by:

$$\hat{P}^{f}_{R,j}(\hat{\pi}_{\neg f}) = \sum_{r \in R} \frac{\exp\left(\frac{-\beta(\mathsf{N}_0 + \hat{I}^{f}_{j}(\hat{\pi}_{\neg f}))}{\mathsf{P} d^{-\alpha}_{r,j}}\right)}{\prod_{r' \in R \setminus \{r\}} \left(1 - \left(\frac{d_{r,j}}{d_{r',j}}\right)^{\alpha}\right)} \tag{1.13}$$

Note that the state of flow is R, a subset of cooperative transmitters. Then the stationary distribution of a node $j \in \mathcal{P}_f$ is given by:

$$\hat{\pi}_f(j) = \sum_{R \subseteq \mathcal{P}_f : j \in R} \hat{\pi}_f(R) \tag{1.14}$$

In the Markov chain for an individual flow f, the state transition probability $\mathbf{P}_{R,R'}$ from $R \subseteq \mathcal{P}_f$ to $R' \subseteq \mathcal{P}_f$ such that $R \subseteq R'$ and $v_{\mathrm{d}(f)} \notin R$, is defined by:

$$\hat{\mathbf{P}}^f_{R,R'}(\hat{\pi}_{\neg f}) \triangleq \prod_{v \in R' \setminus R} \hat{P}^f_{R,v}(\hat{\pi}_{\neg f}) \cdot \prod_{v' \in \mathcal{P}_f \setminus R'} \left(1 - \hat{P}^f_{R,v'}(\hat{\pi}_{\neg f})\right) \tag{1.15}$$

To solve the fixed-point $(\hat{\pi}_f : f \in \mathscr{F})$, we can rely on a similar iterative approach as for the case of opportunistic forwarding.

Theorem 1. *The throughput obtained from the approximate fixed-point model (opportunistic/cooperative) is a lower bound to the corresponding actual throughput of the Markov chain model:*

$$\mathrm{T}_{\mathrm{opp/co}}(f) \geq \hat{\mathrm{T}}_{\mathrm{opp/co}}(f) \tag{1.16}$$

Theorem 1 is important as it helps us appreciate the results obtained by the fixed-point approximation. The above theorem can be proved using Jensen's inequality.

1.6.3 Comparison of Approximation and Simulation

We compare the performance of our approximation models with the simulation results for a 5×5 grid topology. The results in Figure 1.1(b) are obtained for the case of 5 parallel flows, each moving vertically downwards. Flows are given IDs ranging from 1 to 5 starting from one end of the grid to the other. As expected, we find that for both schemes Flows 1 and 5 have maximum and comparable throughput as they experience the minimum amount of interference from other flows. Flow 3 has the minimum throughput because it is situated in the middle and experiences maximum interference. Moreover the throughput of opportunism is greater than cooperation. This is primarily due to increased interference in the cooperative case because of the greater number of transmitters. We note that although the throughput obtained by our approximate model is lower than that obtained by simulation the relative ordering

between opportunistic and cooperative forwarding is preserved. We are currently working on generating confidence intervals for Figures 1.1(a) and 1.1(b).

1.7 Conclusions and Future Work

In this chapter, we use modeling and analysis to investigate the performance benefits of using opportunism and cooperation rather than traditional hop-by-hop, fixed-path routing in multi-hop wireless networks using generic models and under common realistic assumptions. We study general network topologies with multiple flows and formulated Markov chain models to this end. Unlike the single flow case [40], we observe that opportunism outperforms cooperation on average in networks with multiple competing flows. We identify the interference resulting from the larger number of transmissions under cooperative forwarding as a cause for mitigating the potential gains achievable with cooperative forwarding. Lastly, we develop an approximate fixed-point model for analyzing general networks with multiple flows and found that this model produced similar insights regarding the relative performance of opportunistic and cooperative forwarding strategies.

In this work, we have assumed so far that for any link we obtain i.i.d fading in each time slot. In realistic environments, fading will be correlated from one time slot to the next. We plan to incorporate fading correlation in our model and then analyze the performance of opportunistic and cooperative routing. Another question is: How to account for the intra-flow and inter-flow effect when there are multiple concurrent packets within a flow? We have struggled to make progress on this aspect thus far and time permitting we plan to study the multiple packet case as part of our future work.

CHAPTER 2

A MARKOV CHAIN MODEL FOR COARSE TIMESCALE CHANNEL VARIATION

2.1 Introduction

In this chapter we describe a Markov chain model, and its validation, to model the effects of shadowing on the received signal strength. This shadowing model can be used in analyzing performance of wireless network protocols (e.g., for route adaptation, or for video transmission) that adapt their behavior in response to link-level changes at the timescale of seconds.

The underlying physical channel model assumes that the variation in received signal strength due to shadowing is a Gaussian random process with zero mean [33] and has an exponential autocorrelation function, which in turn implies that shadowing follows a First Order Autoregressive AR(1) process. These assumptions (which we test via measurements in a WiMAX network) provide the theoretical framework for adopting a Markov chain model for capturing the effect of shadowing on received power. We divide the entire range of shadowing into a finite number of intervals.

We consider two approaches for determining the transition matrix of the Markov chain: *(i) a parsimonious model-based approach* in which we use the lognormal distribution of shadowing and its exponential autocorrelation to derive expressions for the transition probabilities; this approach is parsimonious as the transition probabilities are dependent only on the variance (σ^2) and the exponential autocorrelation coefficient (ρ) of shadowing; *(ii) an empirical approach* in which transition probabilities are determined from the empirical frequency (taken from measurement traces) of moving from one state to another. We perform signal strength measurements in a

WiMAX network and validate the assumptions of the Markov model, and its predictions (steady state and transient state performance), using these measurements.

The rest of the chapter is organized as follows. In Section 2.2, we discuss related work. We describe our Markov chain model in Section 2.3 and describe two approaches for deriving its transition matrix in Section 2.4. The assumptions of the model are validated in Section 2.5 while a comparison of the experimental and analytical results are presented in Section 2.6. We finally conclude the chapter in Section 2.7.

2.2 Related Work and Applications

There is a great deal of research on developing Markov chain models for wireless channels, with the earliest work in this area being the simple, two-state model proposed by Gilbert and Elliot [12, 14]. Most previous works concentrate on the milliseconds timescale and model the variation of multipath fading. We discuss several of then here and highlight our contributions. In [52], a range of signal-to-noise ratio (SNR) values represents a state in the Markov chain. Based on this assumption the authors provide analytical expressions for the state transition probabilities and error probabilities in each state. In [60], the authors investigate the accuracy of a first-order Markov model for the success/failure of data blocks. A detailed survey of various channel models along with a description of their evolution over time is available in [36]. Our work differs from these existing Markov chain models for wireless channels in the sense that we concentrate on modeling channel variations at a much coarser time granularity, typically in the order of a few seconds and use shadowing to construct our model. We also validate our assumptions and results obtained from the model using data collected via real world experiments in a variety of different settings.

We next survey literature specifically focused on characterizing the properties of shadowing. A thorough description of the different random processes causing variation in the received signal strength over the wireless channel is available in [33, 49].

The lognormal nature of shadowing has been reported in [33, 55] and other prior work. [16] was the seminal paper describing the autocorrelation of shadowing as being exponentially distributed.

Recent research has proposed refined versions of the autocorrelation depending on the environment. In [55], the authors propose a new autocorrelation model for shadowing in urban environments based on data collected in a Chinese city. The correlation properties of shadowing for an indoor channel have been studied in [19, 45]. The authors in [19] observed that shadowing is very environment-specific and that correlation can be found in well-separated links if their environment is similar. Oesteges *et.al* perform an empirical characterization of the received power over a wireless channel in [31] for the outdoor-to-outdoor and indoor-to-indoor environment. They introduce several new aspects specific to multi-user distributed channels and also suggest that shadowing be divided into two components: a static and a dynamic one. Thus, while previous research on shadowing has focused primarily on the underlying process and on studying and characterizing the different properties (distribution, autocorrelation, cross-correlation) of shadowing itself, our work in unique in that we construct a Markov chain model assuming the lognormal distribution and exponential autocorrelation of shadowing.

One of the most useful applications for this modeling work is the scheduling of multiple video streams over a 4G/WiMAX network with the goal of minimizing the number of playout stalls. Other applications where coarse timescale channel modeling might be useful are block-based bit rate adaptation and discontinuation prediction in mobile ad-hoc networks.

2.3 A Shadowing-based channel model

In this section we describe the Markov chain channel model and derive its transition matrix. Let d, α, d_0 be the transmitter-to-receiver separation, the path loss

coefficient and the close-in reference distance respectively. The received power $P_r(d)$ in [dBm] [33] is given by

$$P_r(d)[dBm] = \bar{P}_r(d_0) - 10\alpha \log \frac{d}{d_0} + X \tag{2.1}$$

where $\bar{P}_r(d_0)$ is the average received power at the reference distance d_0 while the second term captures the logarithmic dependence on distance. As noted earlier, shadowing is modeled as a Gaussian random process with mean zero and exponential autocorrelation function [16]. Let X denote the shadowing at any time t; it is assumed to be a Gaussian random variable with mean 0 and variance σ^2 in [dB]. Let X_i and X_{i+n} be the shadowing samples at time i and $i+n$ respectively. The temporal autocorrelation coefficient between X_i and X_{i+n} is given by,

$$\rho_n = \frac{\mathbb{E}[X_i X_{i+n}]}{\sigma^2} = e^{-\frac{n\delta t}{\tau}} \tag{2.2}$$

Let $\rho = e^{-\frac{\delta t}{\tau}}$, and so $\rho_n = \rho^n$. The exponential autocorrelation function implies that the random process is a first-order autoregressive AR(1) process, and therefore

$$X_i = \rho X_{i-1} + (1-\rho)e_i \tag{2.3}$$

where e_i is Gaussian random variable with mean zero and variance σ_e^2. Further e_i and X_{i-1} are independent of each other. X_i being an AR(1) process also implies that shadowing is a Markovian process [53] as the distribution of X_i given X_{i-1} is the same as X_i given X_{i-1}, X_{i-2}....,X_1. This fact is also clear from (2.3) as X_i is only dependent on X_{i-1}.

To construct the Markov chain model, the entire range of shadowing is partitioned into N intervals, $(A_0, A_1....A_N)$, where A_0 and A_N correspond to $-\infty$ and ∞ respectively. Let Y_i denote that the X value is between A_{i-1} and A_i. Therefore $\{Y_i\}$ are the

states of the Markov chain. We now determine the transition probability P_{ij},(i.e. the probability of transitioning from range Y_i to range Y_j) by the parsimonious model-based and empirical approaches.

2.4 Determining the Transition Matrix

In this section we describe the analytical and empirical approaches for determining the transition matrix of the Markov model for shadowing.

2.4.1 Analytical Approach

From the previous section, we know that shadowing (X) is normally distributed and that it is Markovian (2.3). We now determine the state transition probabilities ($P'_{ij}s$,) and begin by stating the following lemma. Lemma 1 can be easily proved using the Cramer-Wold device.

Lemma 1. *Two consecutive shadowing samples are jointly Gaussian*

To calculate the transition probability P_{ij}, we must determine the probability of transitioning from range Y_i to range Y_j at any time step k. X_k and X_{k-1} being jointly Gaussian implies that $X_{k+1}|X_k \sim N(\rho x_k, \sigma^2(1-\rho^2))$. Moreover we have that $X_k \sim N(0, \sigma^2)$. Therefore, we have $P_{ij} = \frac{\int_{Y_i}(\int_{Y_j} f_{X_{k+1}|X_k}(x_2|x_1)dx_2)f_{X_k}(x_1)dx_1}{\int_{Y_i} f_{X_k}(x_1)dx_1}$

As the distributions of $X_{k+1}|X_k$ and X_k are Gaussian, $\int_{Y_j} f_{X_{k+1}|X_k}(x_2|x_1)dx_2$ and $\int_{Y_i} f_{X_k}(x_1)dx_1$ can easily be calculated using error functions. The absolute value of P_{ij} can then be numerically calculated, as the integral in the numerator can be easily solved using a mathematical package such as MATLAB, once the values of ρ and σ have been determined.

2.4.2 Empirical Approach

The transition matrix can also be determined by performing signal strength measurements at the receiver in experiments conducted over any desired network. The first task is to extract the shadowing values by eliminating the deterministic distance

dependent path loss. We then determine the states of the Markov chain to which each of the shadowing values correspond to. We then count the transitions from each state to every other state to determine the transition matrix empirically.

We determine the parameters (σ, ρ) needed for the analytically-determined transition matrix and the directly observed transition probabilities P_{ij} in the empirical transition matrix by conducting experiments over a WiMAX network and extracting the shadowing values.

2.5 Validating the Model

We collected data under varying levels of user mobility (pedestrian and vehicular) for experiments carried out over a WiMAX network at WINLAB in New Jersey. Channel quality measurements were collected continuously by transmitting data from a base station and receiving them on a laptop. Distance variation from the base station outdoors was captured by using a GPS device attached to the laptop. Our goal is to obtain the received signal strength measurement at the beginning of each second. We consider a time window of 50 ms at the beginning of every second and average the received power in this time window to eliminate any fast fading effects; thus we obtain received power samples one second apart from each other. The shadowing samples were extracted by observing the deviation of the received power samples from the log distance relation. In all, three vehicular and two pedestrian traces were collected, each having a duration of approximately 8 minutes.

We use the *Kolmogorov-Smirnov* goodness of fit test to determine the normality of shadowing for the traces collected. Let σ^2_{sam} denote the variance of the collected samples for any trace considered. The null hypothesis is the following: The samples are drawn from a normal distribution having mean 0 and variance σ^2_{sam}. Our tests failed to reject the null hypothesis at any acceptable level of significance for both the vehicular and pedestrian traces. The smoothed probability distribution obtained for one of the vehicular traces using the kernel density estimation method and the

corresponding normal distribution are shown in Figure 2.1(a). The standard deviation for this trace is 4.4 dB.

The temporal autocorrelation function of shadowing for the vehicular traces along with the mean is shown in Figure 2.1(b). We observe that the autocorrelation function does not follow an exponential distribution when the traces are considered individually. Similar results were obtained for the pedestrian mobility case as well.

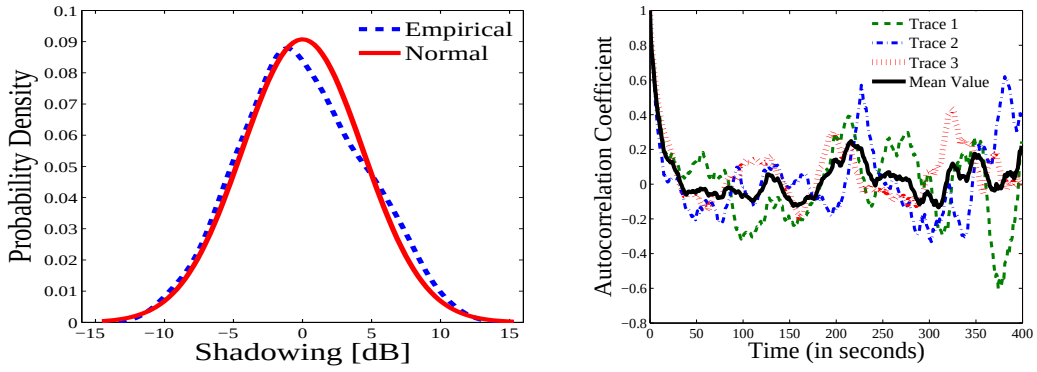

(a) Distribution (b) Autocorrrelation

Figure 2.1. Vehicular: Distribution and Autocorrelation of Shadow Samples

2.6 Results

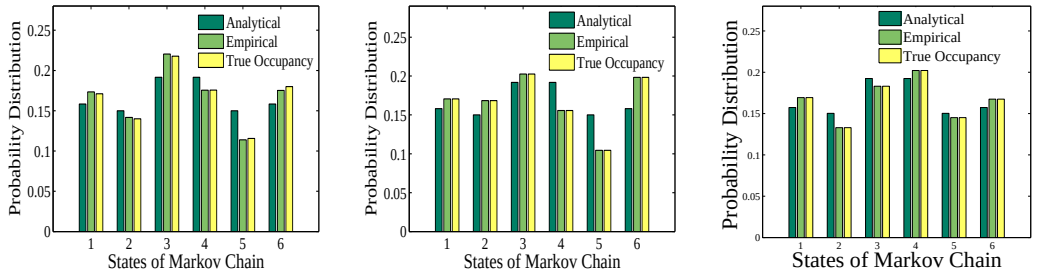

(a) Trace 1 (b) Trace 2 (c) Trace 3

Figure 2.2. Comparison of analytical and empirical steady state occupancies of the Markov chain with the observed occupancy: Vehicular Mobility

In the previous section we tested 1) normality and 2) autocorrelation (exponential form) of shadowing and observed that the shadowing process is not Markovian in reality. In this section we construct the Markov chain and compare the predicted

model-based and empirical steady state performance with the observed shadowing-state occupancies. We construct the Markov chain by dividing shadowing into six intervals: $\{-\infty, -\sigma_{sam}, -\frac{\sigma_{sam}}{2}, 0, \frac{\sigma_{sam}}{2}, \sigma_{sam}, \infty\}$ and determine the model-based and empirical transition matrices for the vehicular and pedestrian mobility traces.

2.6.1 Steady State Behavior

In this subsection we compare the steady state distributions obtained using the analytical and empirical transition matrices with the empirically observed shadowing-state occupancies (True Occupancy). The True Occupancy is calculated by counting the number of shadowing samples in each interval and then normalizing them by the total number of samples. Figure 2.2 shows the steady state behavior for the 3 vehicular mobility traces. Overall, Figure 2.2 shows good agreement in the model-predicted and observed steady state shadowing values, in spite of the lack of exponential autocorrelation evidenced in Figures 2.1. Good agreement in the steady state behavior for the three approaches is also observed in case of pedestrian mobility.

2.6.2 Transient Behavior

In this subsection we focus on the transient state analysis and first determine the empirically observed distribution of transitioning to the different shadowing states as a function of the number of time steps (starting from any state). We once again refer to this as the True Occupancy. We then compare the True Occupancy with the transition probability distribution as obtained from the analytical and empirical transition matrices. As the number of time steps increase the transient behavior will approach steady state.

We study the transient behavior of the Markov chain by comparing the first and second moments (the mean and variance) of the state of the Markov chain obtained by the Analytical, Empirical and (True Occupancy) approaches to determine the closeness of their state distributions. We assign numerical values 1 through 6 for the different states of the Markov chain. For sake of conciseness we show the 2 and

		Mean (2 step)	Variance (2 step)	Mean (5 step)	Variance (5 step)
Trace 1	Anal	3.19	1.99	3.35	2.64
	Emp	3.21	1.88	3.34	2.67
	True	3.08	1.57	3.20	2.28
Trace 2	Anal	3.19	1.99	3.35	2.63
	Emp	3.17	1.95	3.30	2.77
	True	3.29	1.89	3.50	2.88
Trace 2	Anal	3.17	1.80	3.30	2.54
	Emp	3.29	1.94	3.42	2.66
	True	3.16	1.19	3.47	2.47

Table 2.1. Vehicular Mobility: Transient State Behavior

5 time step transitions from state 3 in Tables 2.1 for the vehicular traces. From Table 2.1 we observe that the mean and variance obtained by the analytical and empirical methods are close to the true occupancies. Similar inferences can be drawn for other initial states as well. We performed the same comparisons in the pedestrian mobility scenario, and observed that the performance of the analytical and empirical methods are comparable to one another. But unlike the vehicular mobility case, their performance is not that close to the True Occupancy.

We note here that the after about 25 steps, the probability distribution obtained by the analytical and empirical transition matrices from any state reaches very close (5%) to the steady state distribution for all the vehicular and pedestrian mobility cases.

2.7 Conclusion and Future Work

In this chapter we have developed and validated a finite-state Markov chain channel model to capture wireless channel variations due to shadowing. We obtain the Markov chain transition matrix in two ways: (i) via a two parameter parsimonious modeling approach; (ii) via an empirical approach. The model validation for experiments performed in an WiMAX network showed that the assumption that the variation in received signal strength due to shadowing had a lognormally distributed

random variable was a good one, but that the assumption of an exponential autocorrelation function was violated. Nonetheless, the Markov chain model showed good agreement between the model-predicted and observed values of shadowing for both the steady state and transient behavior.

We are currently trying to understand the reasons for the non-exponential autocorrelation function of shadowing. As a first step, we plan to check the stationarity of the traces. We also plan the test the effectiveness of our model using data collected in other wireless networks. We have embarked on this effort and have already validated the Markov model against publicly available data collected over a multihop mesh testbed deployed at Rice University.

The Markov model described in this chapter does not capture the effect of path loss on the received power and hence can be used for received power prediction, only in scenarios where the path loss is assumed to be constant in the time period of interest. Therefore as an extension of this work we plan to explore the coarse timescale power prediction problem.

We propose adopting a Kalman filtering approach to capture the effect of both path loss and shadowing on the received power. In order to construct a filter for power prediction it is necessary to define the state variables of the system and to model their dependence on one another. We identify the state variables of the filter to be the received power, the distance between sender and receiver and the shadowing. The effect of the shadowing and distance on the received power is governed by a non-linear stochastic equation. The variation in the received power being non-linear, we propose an Extended Kalman Filter (*EKF*)-based estimator for prediction purposes. The ensuing step will be to determine the different parameters of the *EKF*. We then plan to test the effectiveness of the filter using measurements collected over WiMAX and WiFi networks.

CHAPTER 3

QOE MANAGEMENT OF MULTIPLE VIDEO STREAMS

3.1 Introduction

With the deployment of broadband wireless networks, the popularity of multimedia content on mobile devices is expected to increase significantly. The inherent variability of both the wireless channel and the bit rate of compressed videos makes streaming videos on wireless networks a challenging task. The research described in this chapter (which appeared in [41]) investigates how multiple Variable Bit Rate (VBR) videos can be multiplexed over a time-varying wireless channel while still maintaining a good Quality of Experience at the clients.

A wireless video streaming system consists of a video server connected to a base station over a high bandwidth wired backbone link and multiple mobile clients communicating with the base station using a wireless channel. The server stores pre-encoded videos, and upon receiving requests, streams videos to the requesting clients. A video stream is composed of a sequence of frames that the client buffers and plays according to the video's playout time. If a frame is not received by its playout time, the client degrades the displayed video quality or *stalls* the video to wait for more frames to arrive, or both. This work considers systems that stall in response to delayed frames.

Consider the scenario where the rate of each video as well as the rate available to each wireless client varies with time. When the available channel capacity is limited, the server can distribute stalls among the video streams by appropriately scheduling transmissions of video frames to these clients. This chapter considers this multiplexing problem with the goal of minimizing stalls across all mobile clients.

The frame transmission multiplexing scheme we investigate in this chapter makes three contributions. First, we present an epoch-by-epoch framework based on two ideas: (a) We divide the transmission time into *epochs* and use a Markov model to estimate the set of rates available to each wireless client during the next epoch. (b) We define the *playout lead* of a video at a given time as the duration of time the video can be played using only the data already buffered by its client. Since the playout lead plays an important role in determining whether a video stalls in an epoch, we present a fair multiplexing scheme that takes into account the channel rates and maximizes the minimum lead among all videos in an epoch. Second, we show that the optimization problem of maximizing the minimum lead is NP-complete even for two videos. We thus develop and study a fast lead-aware greedy algorithm that is sub-optimal for wireless channels.

The remainder of this chapter is organized as follows. We discuss related work in Section 3.2. We describe the video streaming system and introduce the multiplexing based on playout leads in Sections 3.3 and 3.4 respectively. Hardness results are given in Section 3.5 followed by the greedy algorithm in Section 3.6. We present simulation results in Section 3.7, and finally conclude this chapter Section 3.8.

3.2 Related Work

Although compression techniques reduce the mean bit rate of video streams, they also introduce considerable rate variability over several time scales [13, 34]. Resource allocation for VBR video streaming has been studied extensively for wired networks. Smoothing the video transmission is one of the primary techniques used for reducing the effect of bit rate variability. By pre-fetching some of the initial video frames before their display times, smoothing techniques can minimize the effect of variability in bit rates under various resource constraints, such as peak bit rate, client buffer size, and initial playout delay [21, 32, 44, 46].

Rate allocation for multiple video streams is a well studied problem [15, 27, 37, 47, 56]. [37] investigates minimizing rate variability when transmitting multiple video streams, given the client buffer size in a high-speed wired network. In the RCBR service introduced in [15], the rate of each video is renegotiated at the end of each interval to provide statistical QoS guarantees. [56] presents a call-admission scheme at a statistical multiplexer and bounds the aggregate loss probability. A linear programming model is proposed in [47] to compute a globally optimized smoothing scheme to stream multiple videos. [27] derives bounds on the dropped frames, delay, and buffer requirement that can be obtained by statistically multiplexing VBR streams at the video server by using a two-tiered bandwidth allocation. Although our algorithm performs periodic rate allocation among multiple video streams, our work differs from the above works in two crucial aspects: the primary objective is to fairly manage playout stalls across the videos, and the focus is on a time-varying wireless channel.

Our work is closest to the work presented in [23, 24] for managing stalls. Given the initial playout delay and the receiver buffer size, [24] determines upper and lower bounds on the probability of stall-free display of a video. [23] develops an analytical framework to find the distribution of the number of stalls while streaming a VBR video over a wireless channel. However, unlike our work, both papers consider a single video stream. The problem of transmitting multiple VBR videos from a base station to mobile clients has been studied in [18], but the work focusses on maximizing bandwidth utilization while reducing energy consumption, and does not address the issue of stalling of video playout.

3.3 Streaming system and Channel Model

Consider a video streaming system similar to [23] which simultaneously and separately streams n videos $v_1, \ldots, v_n$ to n clients $1, \ldots, n$ via the base station using a transmission technology such as 4G/WiMAX. A video object is composed of a sequence of VBR frames that are displayed at a constant frame rate by the client. For

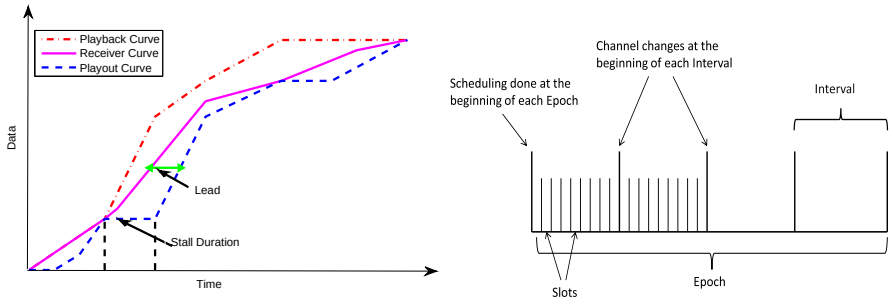

(a) (b)

Figure 3.1. (a) Playback, receiver and playout curves of a video stream (b) Epochs, Intervals, Slots

a video v_i, its *playback curve* $p_i(t)$ specifies the cumulative data contained in the first t time units of the video playout, in order to play the video without interruptions. In other words, $p_i(t)$ is the sum of the sizes of the first $t * F$ frames of the video, where F denotes the frame rate. The playback curve is a characteristic of a video and is independent of the underlying channel. We assume that clients have sufficient buffer space and they buffer frames that have been received but not yet displayed. If the next frame to be displayed is not received within its playout time, the client stalls playout for a *fixed duration* during which it continues to buffer data received from the server. Other *stall-recovery buffering scheme* are studied in [41]. For a client i, its *receiver curve* $G_i(t)$ specifies the cumulative amount of data it has received by time t. The cumulative amount of data played out by time t is given by its *play-out curve* $O_i(t)$. Note that $G_i(t)$ and $O_i(t)$ depends on the the channel conditions and transmission scheme at the base station. In particular, unlike playback curve, the playout curve may vary between different streaming instances of the same video. Figure 3.1(a) shows an example playback, receiver, and playout curve for a client.

We assume time is divided into *epochs*. Each *epoch* is subdivided into intervals (Fig. 3.1(b)). Intervals are further divided into a fixed number of (transmission) *slots* that are allocated to clients. The base station can transmit to at most one client in a slot. We assume the duration of an interval is small enough that the channel state remains unchanged within it. The variation of rates across intervals, as seen at each

client, is independently modeled using a generic discrete-time Markov model given by (R, A) where the possible channel states are identified by the transmission rates $R = (r_1, r_2, \ldots, r_K)$ and A is the transition matrix. Here r_i denotes the number of bits that can be transmitted in a time slot when the channel is in state i [23].

At the beginning of the epoch, clients send their transition matrix, their initial state of the channel and their playout leads to the server. To motivate the allocation strategy, note that a client's current buffer size (in bits) indicates its vulnerability to stalling: the smaller the buffer, the more likely is the occurrence of a stall. However, for VBR videos, buffer size is a poor indicator of this vulnerability since it does not consider the amount of data needed to play the next few frames. On the other hand, the *playout lead* of the video, i.e., the duration of additional time a client can play the video using only its buffered data, takes into account the VBR nature of the video. Therefore in our scheme, within each epoch the server attempts to prevent stalls by maximizing the minimum playout lead.

3.4 Problem Statement

As previously noted, slots are allocated to clients at the beginning of each epoch such that the predicted minimum lead among all videos is maximized at the end of that epoch. We now present our model of this multiplexing problem.

Preliminaries: Let N_{ep}^{in} and N_{in}^{sl} denote the number of intervals in an epoch, and the number of slots in an interval, respectively. Thus the total number slots in an epoch $N_{ep}^{sl} = N_{ep}^{in}.N_{in}^{sl}$. Each video is played at the constant rate of F frames per second. Consider the i^{th} client in a particular epoch. Let I_i be the state vector denoting the probability distribution of channel states at the i^{th} client at the beginning of the epoch. Then, given the Markov channel model, the probability distribution of the channel state at the client at the beginning of the k^{th} interval in the epoch is $I_i A^k$.

Let X_{ik} be the random variable denoting the number of bits that can be transmitted to client i in any slot of the k^{th} interval. Then, its expectation $\mathbb{E}[X_{ik}]$ is the dot

product of $I_i A^k$ and the channel transmission rate vector R. Suppose that the server assigns s_{ik} slots to client i in the k^{th} interval. Then the random variable Y_i for the number of bits transmitted to client i in this epoch can be expressed as $\sum_{k=1}^{N_{ep}^{in}} s_{ik} X_{ik}$. From linearity of expectation, $\mathbb{E}[Y_i] = \sum_{k=1}^{N_{ep}^{in}} s_{ik} \mathbb{E}[X_{ik}] = \sum_{k=1}^{N_{ep}^{in}} s_{ik} \mathbb{E}[I_i A^k R]$.

Playout Lead: The playout lead of a video at a given time is the additional duration of time that the video can be played out using only data currently in the client buffer. Therefore, the playout lead is equal to the number of complete frames in the client buffer divided by the frame rate F. At the beginning of the epoch, let o_i and g_i denote the amount of time for which the video has been played out at the client i, and the amount of time for which the data required for the playout has been received at the client, respectively. (The values of o_i and g_i can be computed from the calculation in the previous epoch, and the video playout and receiver curves.) Thus, the playout lead of the video i at the beginning of this epoch is $g_i - o_i$, and this value is known at the beginning of the epoch. Let L_i be the random variable denoting the playout lead of the video at the end of this epoch (assuming that the video is stalled during the epoch), and V_i be the random variable denoting the number of additional frames that can be *completely* received by the end of this epoch. Then, $L_i = g_i - o_i + (V_i/F)$.

Inverse Playback Curve: For an epoch, we now define a deterministic function that maps the number of bits received to the number of *complete* frames received. The *inverse (frame) playback curve* Φ_i for each video i is defined as follows: if b bits of video i are transmitted in this epoch, then the number of complete frames that are received increases by $\Phi_i(b)$ at the end of the epoch. Thus, $V_i = \Phi_i(Y_i)$. (Note that partially transmitting a frame does not increase the lead of the video.) The inverse playback curve can be easily computed from the video frame sizes.

Estimating $\mathbb{E}[V_i]$ from $\mathbb{E}[Y_i]$: As g_i and o_i are known constants at the beginning of an epoch, $\mathbb{E}[L_i] = g_i - o_i + \mathbb{E}[V_i]/F$. Unfortunately, since the video frame sizes can vary widely, the mapping Φ_i from Y_i to V_i is non-linear, and hence, we cannot

easily obtain $\mathbb{E}[V_i]$ from $\mathbb{E}[Y_i]$. Therefore, we approximate $\mathbb{E}[V_i]$ by $\Phi_i(\mathbb{E}[Y_i])$. Thus, $\mathbb{E}[L_i] \approx g_i - o_i + (1/F)\Phi_i(\mathbb{E}[Y_i]) = g_i - o_i + (1/F)\Phi_i(\sum_{k=1}^{N_{ep}^{in}} s_{ik}\mathbb{E}[I_i A^k R])$.

Lead-based Multiple Video Transmission (LMVT) problem: Our aim, at the beginning of an epoch, is to assign slots with the goal of maximizing the minimum expected lead at the end of the epoch. This problem can be expressed as follows:

Objective: $Max\ Min\{\mathbb{E}[L_1], \ldots, \mathbb{E}[L_n]\}$

subject to the constraints:

1. $\sum_{i=1}^{n} s_{ik} = N_{in}^{sl}, \forall k \leq N_{ep}^{in}$
2. $s_{ik} \geq 0\ , \forall i \leq n, \forall k \leq N_{ep}^{in}$

3.5 Hardness Result

We now investigate the LMVT problem described in the previous section. We first reformulate the problem as a combinatorial problem. (We assume that slots in an epoch are numbered sequentially from 1 to N_{ep}^{sl}.) At the beginning of an epoch, the video of the i^{th} client has an initial lead of $l_i = g_i - o_i$ seconds; i.e., it has received the data corresponding to the $F * l_i$ frames after the last played frame. Let r_{ij} be the expected number of bits of video that can be transmitted to client i in slot j. Thus, $r_{ij} = \mathbb{E}[I_i A^k R]$, when slot j belongs to interval k. Given the above input, we need to find a slot allocation that maximizes the minimum expected playout lead among all videos at the end of the epoch. *We show that the decision version of LMVT is NP-complete: given a constant L, does there exist a slot allocation such that every user has a lead of at least L seconds at the end of the epoch?*

We show the NP-completeness by reduction from the subset-sum problem [10] and show that it holds for even two videos. *For a constant number of videos, we designed a pseudo-polynomial time algorithm to optimally solve LMVT using dynamic programming.* But this algorithm requires long running time when the number of videos is high.

3.6 A Lead-Aware Greedy Algorithm

THe LMVT problem being hard, we present a fast lead-aware greedy algorithm for it. Starting with the initial playout leads of the videos and all the slots in the epoch, the greedy algorithm allocates slots one by one as follows. In each iteration, the algorithm selects a video i with the minimum lead, such that video i has the lowest id among the videos with the minimum lead. Then the algorithm allocates client i a slot j in which client i has the highest rate r among all available slots. Before moving to the next iteration, slot j is marked unavailable for all videos, and the lead of client i is increased corresponding to the transmission of r bits to video i using the inverse playback curve Φ_i. The algorithm iterates until there are no available slots in the epoch. (Recall that the lead in this algorithm refers to the *expected* value of the lead random variable.) Note that the client with the minimum lead that is selected by the algorithm may change between any two slot allocations. Hence, the algorithm allocates the slots one by one even though each client's channel condition is modeled as remaining unchanged within an interval. To motivate our choice of the above greedy algorithm, we now show that the algorithm is optimal for LMVT when each client's channel condition does not change within an epoch (but different clients may have different rates).

Lemma 2. *If the rate of each client does not change within an epoch, the greedy algorithm yields an optimal solution for LMVT.*

The sketch of the proof is as follows. As the rate of a client i does not change within an epoch, each slot allocated to the client i provides a constant number of bits, say r_i. The greedy algorithm simply chooses the client i that has the lowest id among the clients with the minimum lead, and selects the next available slot and allocates it to i. The proof of optimality is by induction on the number of allocated slots.

3.7 Simulation Results

3.7.1 Experimental Setup

To demonstrate the efficacy of the greedy algorithm, we perform trace-based experiments. Our evaluation uses two types of traces:

(i) VBR Video Traces describing the variation in the frame sizes of videos for emulating video playouts. We use the publicly available MPEG-4 *VBR Video Traces* [2, 39] in our experiments. The videos are played out at a constant frame rate of 30 frames per second. We perform experiments with video traces encoded in Common Intermediate Format (CIF). All evaluation is performed assuming that a group of 8 different videos is being streamed simultaneously to 8 different users over a wireless channel.

(ii) User-Level Wireless Channel Traces which describe the rates received by various users in every interval of each epoch to emulate real wireless channel conditions. To generate *User-Level Wireless Channel Traces* we collect signal strength measurements over a WiMAX network deployed in WINLAB at Rutgers University. During our trace collection, the base station was made to continuously transmit data packets, and signal strength (RSSI) was recorded; we performed the measurement at the receiver (a laptop) under vehicular and pedestrian mobility. We use the mapping between the Modulation and Coding Schemes (MCS) and the SINR values for a WiMAX network provided in [1] to generate the Markov Chain for modeling wireless channel state transitions from one interval to the next. We choose interval and epoch durations to be 1 and 10 seconds respectively in our experiments.

3.7.2 Sample Results

In this section we provide some sample illustrative results showing the distribution of stalls as a function of the number of slots in an interval (keeping the interval duration constant) for both vehicular and pedestrian mobility scenarios. Using the steady state probabilities of the Markov model, one can compute the expected number of bits received per slot. By varying the number of slots in an interval we are

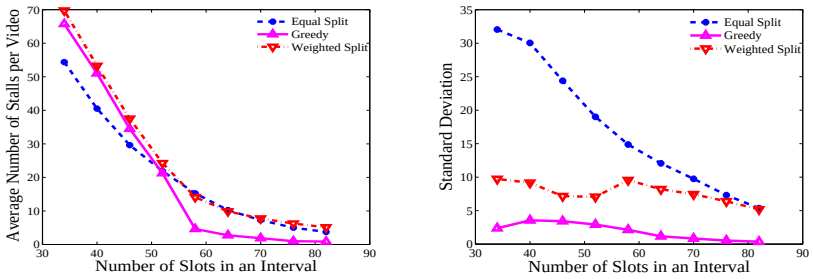

(a) Average number of stalls (b) Fairness

Figure 3.2. Vehicular: Distribution of stalls

essentially varying the total resource (in terms of bandwidth) that is available at the base station.

We compare the performance of the greedy algorithm against two baseline approaches: the equal-split and the weighted-split algorithms. In the equal-split approach, we divide the number of slots available in every interval equally among all the users. In the weighted-split approach, the total number of slots in any interval is divided in proportion to the mean bit rate of the individual video streams. While allocating slots, these two algorithms neither consider the playout lead nor the wireless channel variability, and hence, we expect them to be unfair compared to our greedy strategy.

Figure 3.2 presents the variation of the average number of stalls for three multiplexing algorithms: equal-split, weighted-split and greedy for the vehicular mobility case. The average and over-provisioned scenarios are of interest and we observe that the greedy algorithm outperforms the other two approaches in terms of the average number of stalls per video and the standard deviation of the number of stalls (fairness criterion). In these scenarios we observe that the greedy algorithm reduces the number of stalls by a factor of 3 to 4 when compared to equal-split and weighted-split. We obtain similar results for the pedestrian mobility experiments as well. Overall, we observe that the greedy algorithm gives the best performance both in terms of reducing the average number of stalls per video and evenly distributing the stalls among the videos for both vehicular and pedestrian mobility scenarios.

3.8 Conclusion and Future Work

In this chapter, we presented a greedy multiplex transmission scheme based on a fairness criterion of maximizing the minimum playout lead to manage stalls for multiple video streams that are transmitted over a time-varying bandwidth-constrained wireless channel. We demonstrated that the greedy algorithm is fair and is also capable of minimizing the average number of playout stalls.

We next list our future work, some of which is already underway.

1. In our current formulation, if some client has a poor channel condition for a protracted period of time, the performance of the entire system may be degraded. We have started working on this and observe that a simple strategy of restricting the maximum number of slots allocated to a given client is sufficient for improving the overall performance of the system.

2. We are also testing the robustness of our system for a mixture of pedestrian and vehicular users, different sets of videos and epoch lengths.

3. An implementation of the optimal pseudo-polynomial dynamic programming algorithm is underway and we plan to test its performance against the greedy algorithm for a small number of videos. We are also working on obtaining lower bounds for the average number of stalls experienced by the mobile clients.

4. Our current formulation maximizes the minimum expected lead in playout time in order to reduce the number of playout stalls. In future, we plan to extend the work to address number of playout stalls directly.

CHAPTER 4

OPTIMIZING CONTROL OVERHEAD FOR POWER-AWARE ROUTING

4.1 Introduction

The overhead of gathering state/control information (e.g., link states, node location, queue length) can be significant in an ad-hoc wireless network, where bandwidth is limited and network structure and state may change frequently. In such dynamic scenarios, it may still be advantageous to collect state information, if the decrease in available path bandwidth as a result of state gathering overhead is more than compensated for by better scheduling decisions. Efficient bandwidth use is not the only metric of concern in ad hoc networks; since nodes are typically battery powered, minimizing power consumption is also important.

In this chapter, we analyze the tradeoff between amount of state information collected (at what precision, how often?) and overhead incurred, and the resulting performance (end-to-end power consumption for data and control traffic) in wireless networks while providing goodput guarantees. We develop an information-theoretic, bounding approach to analyze the tradeoff between the amount of signaling overhead incurred in path selection in a MANET with time varying wireless channels and the application-level throughput and end-to-end power expended on the selected path.

4.2 Related Work

Most prior work characterizing the impact of control overhead on performance in wireless networks has relied on simulation [9, 17, 20] or analysis of specific topologies [48]. In [9, 17] the authors compare the overhead, packet delivery ratio and delay

of OLSR and AODV in MANETs and VANETs via simulation. Most theoretical study characterizing the overhead of routing protocols in MANETs has been done by Abouzeid *et.al* [51, 54, 57, 58]. Zhou and Abouzeid [58] mathematically analyze the overhead of reactive routing protocols and estimate the overhead associated with route discovery and route failure. Their analysis is developed in the context of an unreliable network modeled by: 1) an unreliable Manhattan (i.e., degree 4) grid and 2) a random Poisson point distribution of nodes each having equal coverage radius. They validate their numerical results via simulations of regular and random topologies. Information theoretic techniques have been used to obtain lower bounds on memory requirement and routing overhead for hierarchical proactive routing in mobile ad hoc networks in [57].

Our work is closest to [51] where the authors use rate-distortion techniques (an information-theoretic approach) for analyzing the protocol overhead of link state routing in a mobile ad hoc network. They then proceed to derive lower bounds on the minimum bit rate at which a node must receive link state information in order to route data packets with a guaranteed delivery ratio. We differ from the above mentioned works because we consider the path selection problem and are interested in understanding the tradeoff between control overhead and power consumption while providing goodput guarantees.

Power consumption in wireless networks is also a well explored field [3, 26, 50]. In [3] the authors consider the problem of joint routing, scheduling and power control in wireless networks and provide an approximate algorithm with performance guarantees to address it. Liu *et.al* [26] study the optimal power allocation scheme which maximizes the throughput with delay and average power consumption constraints. Network lifetime maximization for an arbitrary data-gathering tree of wireless nodes has be explored in [50] and the authors propose an optimal binary search algorithm for power allocation to achieve the objective. The primary difference between existing literature on power optimization and our work is that we are interested in determin-

ing the optimal sampling frequency and number of bits for encoding samples so as to minimize the power dissipation while maintaining a fixed goodput.

4.3 Problem Statement

We consider a network of n nodes with multiple source-destination pairs. We assume each source has m disjoint paths to the destination with k links on each path and that time is divided into intervals. At the beginning of each interval, each source collects 'noisy' estimates about the links in the network. By 'noise' we refer to the quantization error arising from finite precision representation of link states. The link state estimates characterize the (time-varying) effect of shadowing on the received power. We use the information-theoretic rate-distortion approach to quantify this noise in link state measurements - as we use more bits to encode link state, the fidelity of the estimates increases, but the control overhead also increases. Moreover, each source also requires a fixed amount of goodput, which is defined as the total throughput (including control and data) minus the control overhead. The source's goal is to select a path i among the m paths such that the power consumed in the interval is minimized. The problem we address is the following: *At what time granularity should links be sampled and at what rate (bits) should link values be encoded such that the expected power in any interval is minimized subject to a fixed source-to-destination goodput constraint?*

4.4 Approach

In our model these link state estimates characterize the (time-varying) effect of shadowing on the received power. Shadowing is assumed to be a lognormally distributed random process (in dB it is normally distributed) [33]. Consider any sampling interval and let t be a time of interest in that interval, $0 \leq t < T_s$. Let us consider the i^{th} path and the j^{th} link along this path at some time t. $X_{ij}(t)$ represents the Gaussian distributed shadowing process with mean $\mu = 0$ and autocorrelation func-

tion $R_X(\tau) = \sigma^2 e^{-\lambda\tau}$ [16]. Links are sampled every T_s and hence obtain $\hat{X}_{ij}(0)$ at the beginning of each sampling interval where $\hat{X}_{ij}(0)$ are finite precision representation of $X_{ij}(0)$. The number of bits used to encode the values of $X_{ij}(0)$ determines the closeness of $\hat{X}_{ij}(0)$ to $X_{ij}(0)$ i.e., the inaccuracy in $\hat{X}_{ij}(0)$ decrease as more bits are used for encoding. If ϵ is the noise or quantization error then,

$$\hat{X}_{ij}(0) = X_{ij}(0) + \epsilon \tag{4.1}$$

We model ϵ as Gaussian noise with mean 0 and variance σ_e^2 [30]. We consider that all the link state values are encoded together and sent to the source. We thus use rate-distortion techniques to upper bound σ_e^2.

As mentioned earlier, the source desires a goodput G. Let C_t and C_b be the total throughput (control and data) and control overhead respectively. Therefore we have $C_t = G + C_b$. We note that we do not account for the power consumed for obtaining the raw samples in this work; we only consider the power expended in sending the samples back to the source. Let $P_i(t)$ be the transmitted power along the i^{th} path at time t to achieve a total throughput C_t. The minimum power problem is to determine the sampling interval T_s and the distortion D such that over all possible instantiations of link estimates the expected power consumed (for transmitting both control and data) in any sampling interval to achieve a goodput requirement G is minimized and can be be formally stated as

$$\min_{T_s,D} \mathbb{E}\{\min_i \frac{1}{T_s} \int_0^{T_s} \mathbb{E}[P_i(t)|\hat{X}_{i1}(0)\hat{X}_{i2}(0).....\hat{X}_{ik}(0); T_s, D]\}$$

subject to the constraints:

$$C_t = G + C_b$$

4.5 Ongoing Work

In this section we describe the work that we are currently pursuing. A first version of this work was recently submitted to IEEE Infocom [42].

1. Following [51], we use information theoretic rate-distortion techniques to model the minimum overhead for gathering link state information. We use the Shannon's formula to associate the power consumed to the throughput C_t. Our objective is to leverage the above facts to reduce the optimization problem to achieve a numerically computable solution.

2. We are currently studying the sampling interval - number of bits per sample tradeoff numerically. We are also investigating the dependence of parameters like number of nodes, number of links on path and shadowing correlation on the optimum sampling interval and the number of bits per sample.

3. We also plan to simulate a network with varying link states and compare simulation to numerical results.

4. In our model we make several assumptions such as equal path loss between different pairs of nodes, Gaussian quantization noise, exponential autocorrelation of shadowing. We plan to relax these assumptions and study their impact on the sampling interval - number of bits per sample tradeoff.

5. In our present formulation we assume that link values are encoded anew at the beginning of each sampling interval. We are currently working on relaxing this assumption by leveraging the correlation of the underlying shadowing process and differentially encoding the link samples from one interval to the other.

CHAPTER 5

CONCLUSION

5.1 Thesis summary

The main goal of this thesis is to model the variability of wireless channels and then to exploit this variability in network resource allocation mechanisms and protocols to enhance end-user performance. The first part of the thesis analyzes the performance impact of link quality changes in static networks. In Chapter 1 we model and analyze two classes of routing protocols- opportunism and cooperation under varying channel conditions and in the presence of interfering transmitters. In the second part of the thesis we investigate the impact of both mobility and changing link quality on performance of wireless networks. We first consider the problem of modeling coarse timescale channel variation in wireless networks and develop a Markov Chain model to this end in Chapter 2. In Chapter 3 we explore a video streaming setting and develop a scheduling algorithm which takes into account both channel variability and varying bit rate of videos to improve the users' viewing experience. We examine the tradeoff between sharing network state information (i.e, overhead) and performance (end to end power consumption) in Chapter 4.

The work presented in Chapter 1 has appeared in the Proceedings of the ACITA [8, 40]. The work in Chapters 2 and 3 are available in the Proceedings of Infocom 2012 [41, 43]. Chapter 4 is still work in progress. The research outlined in Chapter 4 was recently submitted to IEEE Infocom.

5.2 Remaining Work Timeline

The remaining work proposed in Chapter 4 will be completed in the next 10 months. Writing the thesis will be done simultaneously with the proposed with completion of the thesis writing requiring an additional couple of months.

BIBLIOGRAPHY

[1] Andrews, Jeffrey, Ghosh, Arunabha, and Muhamed, Rias. *Fundamentals of WiMAX: Understanding Broandband Wireless Networking.* Prentice Hall Communications Engineering and Emerging Technologies Series, 2007.

[2] Auwera, Geert, David, Prasanth, and Reisslein, Martin. Traffic and quality characterization of single-layer video streams encoded with H.264/AVC advanced video coding standard and scalable video coding extension. *IEEE Transactions on Broadcasting 54*, 3 (2008).

[3] Bhatia, Randeep, and Kodialam, Murali. On power efficient communication over multi-hop wireless networks: Joint routing, scheduling and power control. In *IEEE Infocom* (2004).

[4] Biswas, Sanjit, and Morris, Robert. EXOR: Opportunistic routing for wireless networks. In *Proc. ACM SIGCOMM* (2005).

[5] Cacciapuoti, Angela, Caleffi, Marcello, and Paura, Luigi. Design, implementation and evaluation of an effecient opportunistic retransmission protocol. In *Proc. ICUMT* (2009).

[6] Chachulski, Szymon. Trading structure for randomness in wireless opportunistic routing. Master's thesis, Massachusetts Institute of Technology, 2005.

[7] Chachulski, Szymon, Jennings, Michael, Katti, Sachin, and Katabi, Dina. Trading structure for randomness in wireless opportunistic routing. In *Proc. ACM SIGCOMM* (2007).

[8] Chau, Chi-Kin, Seetharam, Anand, Kurose, Jim, and Towsley, Don. Opportunism vs. cooperation: Comparing forwarding strategies in multihop wireless networks with random fading. In *ACITA* (2011).

[9] Clausen, Thomas, Jacquet, Philippe, and Viennot, Laurent. Comparative study of routing protocols for mobile ad-hoc networks. In *MedHoc* (2002).

[10] Cormen, Thomas, Leiserson, Charles, Rivest, Ronald, and Stein, Clifford. *Introduction to Algorithms, Second Edition.* The MIT Press and McGraw-Hill Book Company, 2001.

[11] Ding, Zhiguo, Leung, Kin, Goeckel, Dennis, and Towsley, Don. A relay assisted cooperative transmission protocol for wireless multiple access systems. *IEEE Trans. Communications* (2008).

[12] Elliot, E.O. Estimates of error rates for codes on burst-noise channels. *Bell Syst. Tech. Journal 42* (1963).

[13] Garrett, Mark, and Willinger, Walter. Analysis, modeling and generation of self-similar VBR video traffic. In *ACM SIGCOMM* (1994).

[14] Gilbert, E.N. Capacity of a burst-noise channel. *Bell Syst. Tech. Journal 39* (1960).

[15] Grossglauser, Matthias, Keshav, Srinivasan, and Tse, David. RCBR: a simple and efficient service for multiple time-scale traffic. *IEEE/ACM Trans. Netw. 5*, 6 (1997).

[16] Gudmundson, M. Correlation model for shadow fading in mobile radio systems. *Electronic Letters 27*, 23 (1991).

[17] Haerri, Jerome, Felali, Fethi, and Bonnet, Christian. Performance comparison of aodv and olsr in vanets urban environments under realistic mobility patterns. In *Med-Hoc-Net* (2006).

[18] Hsu, Cheng-Hsin, and Hefeeda, Mohamed. On statistical multiplexing of variable-bit-rate video streams in mobile systems. In *ACM Multimedia* (2009).

[19] Jalden, Niklas, Zetterberg, Per, Ottersten, Bjorn, Hong, Aihua, and Thoma, Reiner. Correlation properties of large scale fading based on indoor measurements. In *IEEE PIMRC* (2007).

[20] Klein, Alexander. Performance comparison and evaluation of aodv, olsr, and sbr in mobile ad-hoc networks. In *IEEE ISWPC* (2008).

[21] Lam, Simon, Chow, Simon, and Yau, David. An algorithm for lossless smoothing of MPEG video. *ACM SIGCOMM Comput. Commun. Rev. 24*, 4 (1994).

[22] Laneman, Nicholas. Cooperative diversity: Models, algorithms and architectures. In *Cooperation in Wireless Networks: Principles and Applications*. Springer, 2006.

[23] Liang, Guanfeng, and Liang, Ben. Balancing interruption frequency and buffering penalties in VBR video streaming. In *INFOCOM* (2007).

[24] Liang, Guanfeng, and Liang, Ben. Effect of delay and buffering on jitter-free streaming over random VBR channels. *IEEE Transactions on Multimedia 10*, 6 (2008).

[25] Liu, Haitao, Zhang, Baoxian, Mouftah, Hussein, Shen, Xiaojun, and Ma, Jian. Opportunistic routing for wireless ad hoc and sensor networks: Present and future directions. *IEEE Comm. Magazine* (December 2009), 103–109.

[26] Liu, Xiangheng, and Goldsmith, Andrea. Optimal power allocation over fading channels with stringent delay constraints. In *ICC* (2002).

[27] Londono, Jorge, and Bestavros, Azer. A two-tiered on-line server- side bandwidth reservation framework for the real-time delivery of multiple video streams. *BUCS-TR-2008-012, Boston University* (2008).

[28] Lu, Mei-Hsuan, Steenkiste, Peter, and Chen, Tsuhan. Video transmission over wireless multihop networks using opportunistic routing. In *Proc. Packet Video Workshop* (2007).

[29] Lu, Mei-Hsuan, Steenkiste, Peter, and Chen, Tsuhan. A theoretical model for opportunistic routing in ad hoc networks. In *Proc. ACM MobiCom* (2009).

[30] Mazo, J. Quantization noise and data transmission. *The Bell Labs Technical Journal* (1968).

[31] Oestges, Claude, Czink, Nicolai, Bandemer, Bernd, and Castigoline, Paolo. Experimental characterization and modeling of outdoor-to-outdoor and indoor-to-indoor distributed channels. *IEEE Trans. On Vehicular Technology 59* (2010).

[32] Ott, Teunis, Lakshman, T. V., and Tabatabai, Ali. A scheme for smoothing delay-sensitive traffic offered to ATM networks. In *IEEE INFOCOM* (1992).

[33] Rappaport, Theodore. *Wireless Communications: Principles and Practice*. Prentice Hall, 2002.

[34] Reibman, Amy, and Berger, Arthur. Traffic descriptors for VBR video teleconferencing over ATM networks. *IEEE/ACM Trans. Netw. 3*, 3 (1995).

[35] Rozner, Eric, Sheshadri, Jayesh, Mehta, Yogita, and Qiu, Lili. SOAR: Simple opportunistic adaptive routing protocol for wireless mesh networks. *IEEE Trans. Mobile Computing 8*, 12 (December 2009), 1622–1635.

[36] Sadeghi, Parastoo, Kennedy, Rodney, Rapajic, Predrag, and Shams, Ramtin. Finite-state markov modeling for fading channels. *IEEE Signal Processing Magazine* (2008).

[37] Salehi, James, Zhang, Zhi-Li, Kurose, Jim, and Towsley, Don. Supporting stored video: reducing rate variability and end-to-end resource requirements through optimal smoothing. *IEEE/ACM Trans. Netw. 6*, 4 (1998).

[38] Scaglione, Anna, Goeckel, Dennis, and Laneman, Nicholas. Cooperative communications in mobile ad-hoc networks: Rethinking the link abstraction. *IEEE Signal Processing Mag. 23*, 5 (September 2006), 18–29.

[39] Seeling, Patrick, Reisslein, Martin, and Kulapala, Beshan. Network performance evaluation with frame size and quality traces of single-layer and two-layer video: A tutorial. *IEEE Communications Surveys and Tutorials 6*, 3 (2004). CIF Video traces availalble at http://trace.eas.asu.edu/mpeg4/index.html and QCIF Video traces available at http://trace.eas.asu.edu/cgi-bin/main.cgi.

[40] Seetharam, Anand, Chau, Chi-Kin, Kurose, Jim, and Towsley, Don. Understanding the benefits of opportunism and cooperation in multihop wireless networks. In *ACITA* (2010).

[41] Seetharam, Anand, Dutta, Partha, Arya, Vijay, Chetlur, Malolan, Kalyanaraman, Shivkumar, and Kurose, Jim. On managing quality of experience of multiple video streams in wireless networks. In *IEEE Infocom* (2012).

[42] Seetharam, Anand, Jiang, Bo, Goeckel, Dennis, Kurose, Jim, and Hancock, Robert. Optimizing control overhead for power-aware routing in wireless networks. In *IEEE Infocom* (2013).

[43] Seetharam, Anand, Kurose, Jim, Goeckel, Dennis, and Bhanage, Gautam. A markov chain model for coarse timescale channel variation in an 802.16e wireless network. In *IEEE Infocom* (2012).

[44] Sen, Subhabrata, Dey, Jayanta, Kurose, Jim, Stankovic, John, and Towsley, Don. Streaming CBR transmission of VBR stored video. In *SPIE Symposium on Voice Video and Data Communications* (1997).

[45] Sharma, Rajesh, and Wallace, Jon. Indoor shadowing correlation measurements for cognitive radio systems. In *IEEE APSURSI* (2009).

[46] Shroff, Ness, and Schwartz, Mischa. Video modeling within networks using deterministic smoothing at the source. In *INFOCOM* (1994).

[47] Stern, Helman, and Hadar, Ofer. Optimal video stream multiplexing through linear programming. In *IEEE International Symposium on Information Technology* (2002).

[48] Tripp, Howard, Hancock, Robert, and Kurose, Jim. Self-tuning routing algorithms. In *ACITA* (2010).

[49] Tse, David, and Vishwanath, Pramod. *Fundamentals of Wireless Communication.* Cambridge University Press, 2005.

[50] Vasudevan, Sudarshan, Zhang, Chun, Goeckel, Dennis, and Towsley, Don. Optimal power allocation in wireless networks with transmitter-receiver power tradeoffs. In *IEEE Infocom* (2006).

[51] Wang, Di, and Abouzeid, Alhussein. Link state routing overhead in mobile ad hoc networks: A rate-distortion. In *IEEE Infocom* (2008).

[52] Wang, Hong Shen, and Moayeri, Nadar. Finite-state markov channel- a useful model for radio communication channels. *IEEE Trans. On Vehicular Technology 44*, 1 (1995).

[53] Wei, William. *Time Series Analysis: Univariate and Multivariate Methods.* Pearson Addison Wesley, 2006.

[54] Wu, Huaming, and Abouzeid, Alhussein. Cluster-based routing overhead in networks with unreliable nodes. In *IEEE WCNC* (2004).

[55] Zhang, Yu, Zhang, Jianhua, Dong, Di, Nie, Xin, Liu, Guanngyi, and Zhang, Ping. A novel spatial autocorrelation model of shadow fading in urban macro environments. In *IEEE GLOBECOM* (2008).

[56] Zhang, Zhi-Li, Kurose, Jim, Salehi, James, and Towsley, Don. Smoothing, statistical multiplexing, and call admission control for stored video. *IEEE Journal on Selected Areas in Communications 15*, 6 (1997).

[57] Zhou, Nianjun, and Abouzeid, Alhussein. Routing in ad hoc networks: a theoretical framework with practical implications. In *IEEE Infocom* (2005).

[58] Zhou, Nianjun, Wu, Huaming, and Abouzeid, Alhussein. The impact of traffic patterns on the overhead of reactive routing protocols. *IEEE Trans on Selected Areas of Comm 23*, 3 (2005).

[59] Zorzi, Michele, and Rao, Ramesh. Geographic random forwarding (GeRaF) for ad hoc and sensor networks: multihop performance. *IEEE Trans. Mobile Computing 2*, 4 (October 2003), 349–365.

[60] Zorzi, Michele, Rao, Ramesh, and Milstein, Laurence. On the accuracy of a first-order markov model for data block transmission on fading channels. In *IEEE ICUPC* (1995).